Reconstructive correction of aberrations in nuclear particle spectrographs

M. Berz, K. Joh,* J. A. Nolen,* B. M. Sherrill, and A. F. Zeller
Department of Physics and Astronomy and National Superconducting Cyclotron Laboratory, Michigan State University, East Lansing, Michigan 48824
(Received 24 August 1992)

A method is presented that allows the reconstruction of trajectories in particle spectrographs and the reconstructive correction of residual aberrations that otherwise limit the resolution. Using a computed or fitted high order transfer map that describes the uncorrected aberrations of the spectrograph, it is possible to calculate a map via an analytic recursion relation that allows the computation of the corrected data of interest such as reaction energy and scattering angle as well as the reconstructed trajectories in terms of position measurements in two planes near the focal plane. The technique is only limited by the accuracy of the position measurements, the incoherent spot sizes, and the accuracy of the transfer map. In practice the method can be expressed as an inversion of a nonlinear map and implemented in the differential algebraic framework. The method is applied to correct residual aberrations in the S800 spectrograph which is under construction at the National Superconducting Cyclotron Laboratory at Michigan State University and to two other high resolution spectrographs.

PACS number(s): 07.75.+h, 29.30.Aj

I. INTRODUCTION

Efficient modern high-resolution spectrographs for nuclear physics usually offer large phase space acceptances, with solid angles of more than 10 msr and energy acceptances of greater than 10%. One such spectrograph is the S800 currently under construction at Michigan State University's National Superconducting Cyclotron Laboratory [1,2]. Such large acceptance, high-resolution spectrographs require careful consideration and correction of aberrations. But because of the large phase space acceptance, aberrations up to seventh order may contribute significantly and affect the resolution.

The large phase space makes the correction process considerably more difficult and complex, and often prevents a complete correction of aberrations in the conventional sense. The conventional correction of aberrations with higher order hardware (sextupoles, octupoles, dipole edge curvatures, etc) will cure second or third order aberrations, but at the expense of inducing large higher order terms. These terms will eventually limit the maximum solid angle and energy acceptance.

It is often possible to circumvent or at least alleviate these problems by using additional information about the particles. In particular, one often measures not only their final positions but also their final slopes by means of a second detector. With this additional information one attempts to retroactively construct the whole trajectory of the particle. This information can be used both for the numerical correction of the quantities of interest, as well as to reveal additional properties such as the scattering angle, which is important in the study of many nuclear processes. Some proposed spectrographs, such as those under construction at CEBAF, will use hardware corrections to reduce aberrations up to fifth order and additionally trajectory reconstruction to meet their design goals [3].

A powerful numerical procedure to calculate a polynomial relationship between measured final coordinates and the quantities of interest is contained in the program MOTER [4,5]. Using magnetic-field specifications and geometry as input, this program relates initial coordinates, selected randomly, to the corresponding final coordinates by numerically tracing each ray through the system. The coefficients of the polynomial are determined by a numerical fit to the data from the ray tracing results. The relevant coefficients to be included in this fitting procedure which are connected to the significant aberrations of the system are chosen by experience and empirical trials, and for reasons of computational expense there are limits to the number of coefficients that can be considered [6]. Such trajectory reconstruction techniques are usually quite involved computationally. In the following, we present a new direct and efficient method based on differential algebraic (DA) techniques, which is also very useful in rapidly evaluating or optimizing spectrograph designs [7].

Recently we have shown that maps of particle optical systems can be computed to higher orders than previously possible using DA methods [8–11]. Furthermore, the techniques also allow the computation of maps for complicated measured fields that can be treated only approximately otherwise. In our particular case, these include the fringe fields of the large aperture magnets required for such particle spectrographs. As soon as the fields are known, it is now possible to compute all the aberrations that occur in a modern high-resolution spectrograph without having to rely on tedious ray tracing.

On the practical side this requires high order codes for the computation of highly accurate maps for realistic fields. The new code COSY INFINITY [7, 12–14] allows such computations in a powerful language environment.

*Present address: Argonne National Laboratory, 9700 South Cass Avenue, Argonne, IL 60439.

It also has extensive and general optimization capabilities, supports interactive graphics, and provides ample power for customized problems, and it contains all the necessary tools for efficient trajectory reconstruction.

II. INVERSION OF TRANSFER MAPS

At the core of the algorithms developed below is the need to invert Taylor transfer maps. It turns out that there is a direct iterative algorithm to perform this task. The algorithm is implemented using the DA software and the driver code COSY INFINITY and, in practice, readily allows the inversion of transfer maps of arbitrary order. We begin the algorithm by splitting the nonlinear Taylor map A_n of order n into its linear first order part A_1 and the purely nonlinear remainder A_n^*:

$$A_n = A_1 + A_n^*. \tag{1}$$

The nth Taylor polynomial of the inverse map, if it exists, is written as M_n. Denoting agreement to order n with $=_n$, which is an equivalence relation, we have $A_n \circ M_n =_n I$; i.e., the composition of the Taylor maps equals the identity to order n. Separating into linear and nonlinear parts, we obtain

$$\begin{aligned}(A_1 + A_n^*) \circ M_n &=_n I \\ \Rightarrow\ A_1 \circ M_n &=_n I - A_n^* \circ M_n \\ \Rightarrow\ M_n &=_n A_1^{-1} \circ (I - A_n^* \circ M_{n-1}).\end{aligned} \tag{2}$$

In the last step use has been made of the crucial fact that because A_n^* is purely nonlinear, to order n the nth order terms in M_n do not contribute to $A_n^* \circ M_n$, and so we have $A_n^* \circ M_n =_n A_n^* \circ M_{n-1}$. So Eq. (2) allows the iterative, order by order computation of M_n in a direct way. We point out that the only requirement is that the linear matrix A_1 be invertible. This is similar as in the case of the implicit function theorem that assures the existence of an inverse in a neighborhood of a point at which the Jacobian of a given function is not singular.

We note that transfer maps of particle optical systems derived from Hamiltonian equations of motion always have a nonsingular Jacobian because of Liouville's theorem and can thus always be inverted.

III. TRAJECTORY RECONSTRUCTION IN THE DISPERSIVE CASE

The result of the computation of the transfer map of the system allows the final coordinates to be related to initial coordinates and parameters. In our case, the relevant coordinates are the positions in the dispersive direction x and the transverse direction y as well as the measures of slopes $a = p_x/p_0$ and $b = p_y/p_0$ and the relative energy deviation $d = \Delta E/E$ of the particles under consideration. Here $\mathbf{p}$ is the momentum and E the energy of the particles. With the subscript i we denote initial ray coordinates and with f final ray coordinates; the partial derivative of final ray coordinates with respect to initial ray coordinates $\partial^{k_1+\cdots+k_5}/\partial r_1^{k_1} \cdots \partial r_5^{k_5} r_{jf}$ is denoted with $(r_j, r_1^{k_1} \cdots r_5^{k_5})$. For example, the second derivative of the final x position with respect to the initial x momentum is (x, aa).

Usually the range of initial x values at the target is kept small because this initial spot size determines the first order energy resolution, which is the ultimate limit of any method correcting aberrations. So the final positions in the focal plane are primarily determined by the energy, and to higher orders also by the initial y position and the initial slopes a_i and b_i.

For the purpose of trajectory reconstruction we now assume that all initial positions x_i in the full transfer map will be small and approximate them by zero. This approximation will ultimately limit the resolution of reconstruction. We obtain the following nonlinear submap:

$$\begin{pmatrix} x_f \\ a_f \\ y_f \\ b_f \end{pmatrix} = \mathcal{S} \begin{pmatrix} a_r \\ y_i \\ b_r \\ d_r \end{pmatrix}. \tag{3}$$

This map relates the quantities which can be measured in the two planes to the quantities of interest a_r, b_r, d_r, which characterize the nuclear reaction being studied as well as the initial position y_i which unaffected by the reaction process and therefore of little interest. The map $\mathcal{S}$ is not a regular transfer map, and in particular its linear part does not have to be *a priori* invertible. In a particle spectrograph with point-to-point imaging in the dispersive plane, the linear part S of the map $\mathcal{S}$ has the following form:

$$\begin{pmatrix} x_f \\ a_f \\ y_f \\ b_f \end{pmatrix} = \begin{pmatrix} 0\,0\,0\,* \\ *\,0\,0\,* \\ 0\,*\,*\,0 \\ 0\,*\,*\,0 \end{pmatrix} \begin{pmatrix} a_r \\ y_i \\ b_r \\ d_r \end{pmatrix}, \tag{4}$$

where the star denotes nonzero entries. Since the system is imaging, clearly (x, a) vanishes, and all the other zero terms vanish because of midplane symmetry. (x, d) is maximized in spectrograph design, and (a, a) cannot vanish in an imaging system because of symplecticity [15]. In fact, to reduce the effect of the finite target, (x, x) is often minimized within the constraints, and so $(a, a) = 1/(x, x)$ is also maximized.

Because of symplecticity, $(y, y)(b, b) - (y, b)(b, y) = 1$, and so we obtain, for the total determinant of S,

$$|S| = (x, d)(a, a) \neq 0. \tag{5}$$

Incidentally, the size of the determinant is a measure of the quality of the spectrograph because the linear resolution is defined as

$$r = \frac{(x, d)}{(x, x) x_t} = \frac{|S|}{x_t}, \tag{6}$$

where x_t is the target thickness or incoherent spot size. So certainly the linear matrix is invertible, and, according to the last section, this entails that the whole nonlinear map $\mathcal{S}$ is invertible to arbitrary order. Thus it is possible to compute the initial quantities of interest to arbitrary order via the map

$$\begin{pmatrix} a_r \\ y_i \\ b_r \\ d_r \end{pmatrix} = \mathcal{S}^{-1} \begin{pmatrix} x_f \\ a_f \\ y_f \\ b_f \end{pmatrix}. \tag{7}$$

Compared to the numerical method, the nonlinear terms in the polynomial are exact and computed directly. Furthermore, the aberration coefficients that are relevant are determined in a straightforward manner and do not have to be guessed, and there are essentially no limitations as to their number.

A closer inspection of the algorithm shows that in each iteration the result is multiplied by the inverse of the linear matrix S. Since the determinant of this inverse is the inverse of the original determinant and is thus small for a well designed spectrograph, this entails that the originally potentially large terms in the nonlinear part of the original map are suppressed accordingly. So, for a given accuracy, this may reduce the number of terms required to represent the reconstruction map. Thus, in the case of trajectory reconstruction, the original investment in the quality of the spectrograph and its linear resolution directly influences the quality of the reconstruction.

The method to determine the reconstruction map $\mathcal{S}^{-1}$ has been implemented in COSY INFINITY [7]. The resolution of the spectrograph using reconstruction is also computed. To this end, an ensemble of rays is selected statistically in the initial phase space and then traced through the system using the forward map. The position and slope measurement errors are simulated by adding statistical noise to the positions and slopes. The resulting positions and slopes are traced through the reconstruction map $\mathcal{S}^{-1}$, and the resulting predicted phase space values are compared with the known original values.

This procedure for evaluating the effect of the intrinsic aberrations of the system and the uncertainties related to detector limitations is very similar to that used in MOTER except that map methods instead of ray tracing are used. Altogether, however, the process of DA reconstruction and statistical evaluation takes a few seconds of computer time on a VAX 3200 and in our case proved to be 100–1000 times faster than in the conventional ray tracing approach.

IV. TRAJECTORY RECONSTRUCTION IN THE ENERGY LOSS MODE

The method outlined in the previous section allows a precise determination of the energy of a particle traversing the spectrograph. This energy is given by the energy before hitting the target plus the change of energy experienced in the reaction. In the study and analysis of nuclear processes, it is this change in energy that is relevant, along with the angular distribution of the products. In many cases, the energy resolution of the spectrograph is substantially better than the energy spread in the incoming beam; hence the resolution of the measurement could be limited by the energy resolution of the beam.

There is a remedy to this fundamental problem, the so-called energy loss mode or technique of dispersion matching [16]. In this technique, the dispersive spectrograph is preceded by another dispersive device, the beam matching section, in such a way that the resulting system is achromatic to first order; i.e., the final positions and slopes of particles do not depend on energy to first order. The solid line in Fig. 1 schematically shows the trajectory of an off-energy particle as a function of position going through the matching section and the spectrograph.

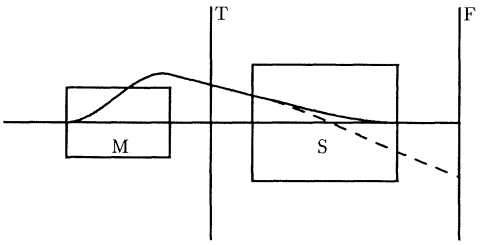

FIG. 1. Principle of dispersion matching. The linear dispersion properties of the matching section M (the beam analysis system) are chosen such that M followed by the spectrograph S becomes linearly achromatic and hence off-energy particles follow the solid line. Particles which experience a change in energy due to interactions in the target T hit the focal plane F at a different location (dashed trajectory).

Besides the energy spread, which is typically about 0.1%, it is assumed that the phase space going through the matching section is small compared to the phase space after the target. This entails that any one energy in the target plane between the matching section and the spectrograph correspond to a relatively small spot in the x direction, the center of which depends on the energy. Similarly, any one energy corresponds to a relatively small spot in the a direction, and the center of the spot again depends on the energy.

The matching system is now optimized such that the size of the spot for a given energy component of the beam, the incoherent spot size, is minimized and the centers x_c and a_c of the incoherent spot in the x and a directions can be described in terms of the beam energy spread d_i as

$$x_c = k_x d_i \ , \quad a_c = k_a d_i, \tag{8}$$

where the matching condition connects the factors k_x and k_a to the matrix elements of the main part of the spectrograph:

$$\begin{aligned} k_x &= (x,x)(a,d) - (a,a)(x,d), \\ k_a &= (a,x)(x,d) - (x,x)(a,d). \end{aligned} \tag{9}$$

To achieve this situation with the beam analysis system may require some aberration correction, but because of the small phase spaces of the beam involved, the task is substantially simpler than it would be for the main spectrograph.

In order to determine a reconstruction map, we now perform an approximation similar to the one in the previous section by assuming that all beam particles are actually located at the energy dependent center of the incoherent spot x_c and neglect the finite width of the spot. In a similar way, we assume that all beam particle slopes a are actually equal to the center of the slope spot a_c. In the vertical direction, we assume that the beam slopes b are all zero, but we do allow for a nonzero spot size

in y direction. Similar to the nondispersive case, it is this incoherent spot size which determines the first order resolution of the system and hence is a limit for the resolution achievable in higher order.

The reaction that is to be studied now takes place at the target plane T in Fig. 1. In the reaction, the slopes a, b of the particle as well as its energy d_i are being changed by the quantities a_r, b_r, and d_r, which are characteristic of the reaction. The range of possible angular changes is much larger than the spread in these values for the beam. So, after the reaction, we have the following approximations:

$$\begin{aligned} x &= k_x d_i, \\ a &= k_a d_i + a_r, \\ y &= y_i, \\ b &= b_r, \\ d &= d_i + d_r. \end{aligned} \tag{10}$$

These five quantities now have to be propagated through the spectrograph proper. In terms of transfer maps, this requires inserting the linear transfer map represented by Eq. (10) into the nonlinear transfer map describing the spectrograph. The result is a map relating the measurable final quantities after the system x_f, a_f, y_f, and b_f to the quantities d_i, d_r, a_r, y_i, and b_r.

Performing the insertion of Eq. (10) into the spectrograph map reveals that as a consequence of the dispersion matching, the final quantities no longer depend linearly on the unknown intial energy d_i. Higher order dependences on d_i usually still exist, but since they contain products of small quantities, they are of reduced importance. In ignoring this higher order influence and setting d_i to zero, a final approximation is performed. Altogether we are left with a map of the following form:

$$\begin{pmatrix} x_f \\ a_f \\ y_f \\ b_f \end{pmatrix} = \mathcal{S} \begin{pmatrix} a_r \\ y_i \\ b_r \\ d_r \end{pmatrix}. \tag{11}$$

Now the situation is similar to the one in the last section: The linear part of this map has the same structure as above, the determinant has the same form, and so we can apply the same techniques and reasoning to find the reconstruction map:

$$\begin{pmatrix} a_r \\ y \\ b_r \\ d_r \end{pmatrix} = \mathcal{S}^{-1} \begin{pmatrix} x_f \\ a_f \\ y_f \\ b_f \end{pmatrix}. \tag{12}$$

Similar to the dispersive case, the method to determine the reconstruction map $\mathcal{S}^{-1}$ has been implemented in COSY INFINITY. The spectrograph resolution is also computed for this technique. Again an ensemble of rays is selected statistically in the phase space before the spectrograph, but now such that center position and slope are correlated to the energy except for a statistical effect determined by the incoherent spot size. To these beam parameters, statistical values for the quantities of interest d_r, a_r, and b_r are added, and the resulting rays are traced through the forward map. Again the position and slope measurement errors, inherent in the focal plane detectors, are simulated by adding statistical noise to the positions and slopes. The resulting positions and slopes are traced through the reconstruction map $\mathcal{S}^{-1}$, and the resulting predicted values for d_r, a_r, and b_r are compared with the known original values. Should it be necessary, it will be straightforward to generalize this method to include the detailed transfer map of the beam analysis system and its possible high order terms.

V. TRAJECTORY RECONSTRUCTION AND CORRECTION OF THE S800 SPECTROGRAPH

The S800 [1] is a superconducting magnetic spectrograph which is under construction at the National Superconducting Cyclotron Laboratory at Michigan State University. The spectrograph and its associated analysis line will allow the study of heavy ion reactions with momenta of up to 1.2 GeV/c. It is designed for an energy resolution of one part in 10 000 with a large solid angle of 20 msr and an energy acceptance of 10%. The spectrograph will be used in connection with the K1200 superconducting cyclotron for beams of protons to uranium with energies up to 200 MeV per nucleon. It is expected to provide unique opportunities for research in various areas, including the study of giant resonances, charge exchange, direct reaction studies, and fundamental investigations of nuclear structure [17].

The S800 consists of two superconducting quadrupoles followed by two 75° superconducting dipoles with y-focusing edge angles. Table I lists the parameters of the system, and Fig. 2 shows the layout of the device. It should be noted that the S800 disperses in the vertical direction, while the scattering angle is measured in the transverse plane. Thus the first order focal plane is two dimensional, with energy measured in one dimension and the scattering angle measured in the other. For recon-

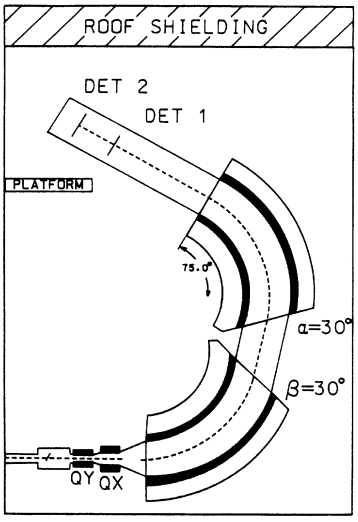

FIG. 2. Layout of the S800 spectrograph.

TABLE I. S800 spectrograph.

Drift	$l = 60$ cm				
Quad	$l = 40$ cm	$G_{max} = 21$ T/m	$r = 0.1$ m		
Drift	$l = 20$ cm				
Quad	$l = 40$ cm	$G_{max} = 6.8$ T/m	$r = 0.2$ m		
Drift	$l = 50$ cm				
Dipole	$\rho = 2.6667$ m	$B_{max} = 1.5$ T	$\phi = 75°$	$\epsilon_1 = 0°$	$\epsilon_2 = 30°$
Drift	$l = 140$ cm				
Dipole	$\rho = 2.6667$ m	$B_{max} = 1.5$ T	$\phi = 75°$	$\epsilon_1 = 30°$	$\epsilon_2 = 0°$
Drift	$l = 257.5$ cm				

structive aberration correction, a second two-dimensional detector is required.

The aberrations of the S800 have been calculated using the program COSY INFINITY [7, 12, 14]. Care was taken to include a detailed treatment of the fringing fields of the system. To this end, the falloff of the dipole field as well as the quadrupole strengths were described by the standard Enge-type functions [18]

$$F(z) = \frac{1}{1 + \exp(a_0 + a_1 z + a_2 z^2 + \cdots + a_5 z^5)} , \qquad (13)$$

where the coefficients a_0–a_5 are adjusted to describe the shape of the fringe field. The information about the field in the magnetic median plane is then used to compute the exact off-plane expansion using standard techniques [12, 19, 20]. For practical purposes it is worth noting that this requires the computation of high order derivatives of the Enge function, a problem for which the differential algebraic techniques again prove helpful.

The equations of motion in their differential algebraic form [8, 12] are now used to compute the exact expansion of the transfer map around the reference trajectory to high orders. The accuracy of this procedure is only limited by the accuracy of the numerical integrator, which in our case is an eighth order Runge-Kutta integrator with automatic step size control [21] to achieve a specified accuracy, which was set to better than 10^{-10}.

The overall accuracy of the fringe field effects is certainly affected by the accuracy with which the Enge function represents the fringe field falloff for the specific element. Since so far no measurements of the dipole and quadrupole fringe fields exist, for the purpose of an advance estimate of the performance of the device we have assumed that the coefficients correspond to those of another magnet [22]. Once field measurements for the dipole exist, the computations will be repeated with the proper values.

In this respect it is important to note that in the fitting process not only the underlying function has to be represented accurately, but also its z derivatives since these derivative to order n couple to the image aberrations to order n. For such estimations of derivatives, it is often not sufficient to use just information in the plane [5]. In our case we plan to measure the fields in additional planes above and below the midplane, and we also plan to measure the first derivative in z direction directly with a moving coil method.

The resulting information will be used to fit a function satisfying Maxwell's equations, and this function will then be used for the computation. We will also attempt to fit the three-dimensional fields by an Enge function in the midplane, demanding that the derivatives as well as the off-plane expansion represent the measured data. At this point it is not clear if the resulting Enge coefficients will be sufficient to represent the field accurately enough over the whole range of interest, and perhaps other methods will be used [5]. The non-fringe-field part of each element is computed using the differential algebraic time propagation operator method discussed in [8, 23], which substantially outperforms a numerical integration method in speed.

We expect that the resulting transfer map to order 7 will represent the actual spectrograph with an accuracy sufficient for the desired resolution. We will verify this independently using experimental ray tracing techniques with individual beams.

The linear resolution of the S800 spectrograph is limited simultaneously by the incoherent spot size of 0.46 mm and the detector resolution which is (somewhat conservatively) assumed to be 0.4 mm and 0.3 mrad full width at half maximum (FWHM) in both planes of the detectors [24]. These two effects limit the energy resolution to about 10 000. Since no hardware correction of higher order aberrations has been incorporated in this design, the map of the spectrograph exhibits rather large aberrations, which if left uncorrected would decrease the

TABLE II. Resolution of the S800 for various correction orders. The resolutions are based on a detector resolution of 0.4 mm and 0.3 mrad FWHM and a rectangular phase space of (±0.23 mm) × (±60 mrad) (x), (±10 mm) × (±90 mrad) (y), and ± 5% (d).

	Energy resolution ($\Delta E/E$)	Angle resolution (1/rad)
Linear resolution	9400	
Uncorrected nonlinear	100	25
Order 2 reconstruction	1500	150
Order 3 reconstruction	6300	600
Order 4 reconstruction	8700	700
Order 5 reconstruction	9100	1300
Order 8 reconstruction	9100	1300

resulting resolution to only little more than 100. In particular, the slope dependent aberrations are contributing substantially, with (x, aa) being the largest.

Using the map of the S800, the trajectory reconstruction was performed to various orders and the resolutions computed following the methods outlined in the previous section. Table II shows the resulting resolutions as a function of the reconstruction order.

The resolution with trajectory reconstruction correction improves with order; with third order reconstruction, about 65% of the linear resolution is recovered, and with fifth order correction, this increases to about 96% of the linear resolution and thus satisfies the design specifications.

Besides the computation of the corrected energy, the two plane reconstruction technique also allows the computation of the angle under which the particle entered the spectrograph which is dominated by the scattering angle. The prediction accuracy for this initial angle reaches about 1300 at fifth order, which corresponds to an angle resolution of about 0.05° (0.75 mrad).

It is worthwhile to study the influence of possible improvements in the detector resolution on the resolution of the spectrograph. For this purpose, the focal plane position resolution was assumed to be 0.2 mm. Since the resolution limit due to the spot size now corresponds to the detector resolution limit, the incoherent spot size was also reduced by a factor of 2. Table III shows the resulting resolutions as a function of the order of the reconstruction. With an eighth order reconstruction, about 90% of the now twice as large resolution is recovered. Note that contrary to the previous operation mode, a third order reconstruction now gives less than half of the linear resolution.

Frequently an increase in the position resolution comes at the expense of increased angle straggling which reduces the maximum angle resolution [24]. To study the properties of the S800 under this scenario, the focal plane angular resolution was decreased by a factor of 2 and the computation performed again. The result in Table IV shows that in this case only about 75% of the linear resolution can be recovered using trajectory reconstruction, representing only a 50% increase compared to the more pessimistic estimate of detector resolution.

TABLE III. Resolution of the S800 for various correction orders for a detector resolution of 0.2 mm and 0.3 mrad FHWM and a reduced phase space of (±0.115 mm) × (±60 mrad) (x), (±10 mm) × (±90 mrad) (y), and ± 5% (d).

	Energy resolution $(\Delta E/E)$	Angle resolution (1/rad)
Linear resolution	19 000	
Uncorrected nonlinear	100	25
Order 2 reconstruction	1 500	150
Order 3 reconstruction	7 900	650
Order 4 reconstruction	14 600	750
Order 5 reconstruction	16 800	1500
Order 8 reconstruction	17 000	1800

TABLE IV. Resolution of the S800 for various correction orders for an increased position detector resolution of 0.2 mm at the expense of a decreased angular resolution of 0.6 mrad. The other parameters are the same as in Table III.

	Energy resolution $(\Delta E/E)$	Angle resolution (1/rad)
Linear resolution	19 000	
Uncorrected nonlinear	100	25
Order 2 reconstruction	1 550	150
Order 3 reconstruction	7 500	550
Order 4 reconstruction	12 500	600
Order 5 reconstruction	14 000	1000
Order 8 reconstruction	14 000	1100

VI. TRAJECTORY RECONSTRUCTION IN MORE EXTREME CASES

In the previous section it became apparent that for the case of the S800 the trajectory reconstruction using the method presented here allows a correction of the device to nearly the linear limit and design specifications; with better detectors and smaller incoherent spot size, even increased resolutions are possible. In this section we want to study more extreme cases which challenge different aspects of the reconstruction method.

For the first example, we consider a spectrograph such as the S800 where the aperture of the magnets in the dispersive plane has to be increased substantially to now accept angles of ±100 mrad and energy deviations of ±10%. The linear resolution is, of course, the same as before, but because of the higher acceptance, the higher order aberrations become substantially larger. This entails that the unreconstructed nonlinear resolution drops to only 35, indicating a fourfold increase in the significance of nonlinear aberrations.

Table V shows that about 90% of the linear resolu-

TABLE V. S800-like spectrograph with increased angular acceptance of 200 mrad and energy acceptance of ±10%, with detector parameters identical to those in Table II.

	Energy resolution $(\Delta E/E)$	Angle resolution (1/rad)
Linear resolution	9500	
Uncorrected nonlinear	35	15
Order 2 reconstruction	320	75
Order 3 reconstruction	1100	400
Order 4 reconstruction	2200	600
Order 5 reconstruction	5700	850
Order 6 reconstruction	7300	1000
Order 7 reconstruction	8500	1000
Order 8 reconstruction	8800	1000

TABLE VI. S800 increased in size by factor 5. The phase space is the same as for the S800 in Table III, the position resolution of the detectors is 0.2 mm, and the angular resolution is assumed to be 0.15 mrad.

	Energy resolution ($\Delta E/E$)	Angle resolution (1/rad)
Linear resolution	95 000	
Uncorrected nonlinear	100	25
Order 2 reconstruction	1 500	300
Order 3 reconstruction	9 700	750
Order 4 reconstruction	32 000	22 000
Order 5 reconstruction	85 000	28 000
Order 6 reconstruction	91 000	29 000
Order 7 reconstruction	93 000	29 000
Order 8 reconstruction	93 000	29 000

TABLE VII. Crude 10-m-radius 90° single dipole spectrograph accepting a phase space of 0.2×300 mm mrad (x), 20×200 mm mrad (y), and $\pm 10\%$ (d). The detector resolution is zero. The linear resolution of 50 000 is almost fully recovered despite aberrations that limit the uncorrected resolution to about 20.

	Energy resolution ($\Delta E/E$)	Angle resolution (1/rad)
Linear resolution	50 000	
Uncorrected nonlinear	20	200
Order 2 reconstruction	800	3900
Order 3 reconstruction	5 400	23 600
Order 4 reconstruction	23 600	63 500
Order 5 reconstruction	43 000	96 500
Order 6 reconstruction	47 000	99 000
Order 7 reconstruction	48 000	99 000
Order 8 reconstruction	48 000	99 000

tion can eventually be recovered, but as might be expected only at higher reconstruction orders. At fifth order, which was sufficient for the normal case, only about half of the resolution is recovered.

The next example illustrates the effect of the sheer size of the device. It represents the S800 scaled up by a factor of 5 in all its linear dimensions. The phase space is assumed to be like in the high-resolution mode of the S800, and so is the position detector resolution. This means the linear resolution is now 5 times larger than in Table III and nearly 100 000. The angular detector resolution is assumed to have increased by another factor of 2. As Table VI shows, the linear resolution is eventually almost fully recovered. Because of the much higher accuracy demand, this requires a seventh order correction. At third order, only the resolution of the original S800 is achieved.

In the final example we want to apply the techniques to a very crude spectrograph: a 90° dipole magnet preceded and followed by a drift equal to its bending radius, a combination which is well known to be imaging in the dispersive plane. In order to obtain high resolutions, the deflection radius is chosen as 10 m. The incoherent spot size is chosen as 0.1 mm, similar to the case of the high-resolution S800; the rest of the phase space quantities are very large. For the sake of argument, the measurement errors are assumed to be zero. The resolutions as a function of reconstruction order are shown in Table VII.

In this example, the reconstructive correction boosts the resolution by a factor of about 2500, illustrating the versatility of the technique for very crude systems.

In extreme cases such as the one here, aside from the unavoidable limitations due to detector resolution and incoherent spot size, the major limitation is the exact knowledge of the fields of the elements, in particular the fringe fields. On the other hand, the layout of the device is rather uncritical; even substantial aberrations can be corrected with the method. This suggests that spectrographs geared towards high-resolution reconstruction should be designed with different criteria than conventional devices. The main aspect being the knowledge of the fields but not their form, one should concentrate on devices for which the fields in space are known very precisely in advance.

Altogether we have developed a new method for the efficient reconstruction of trajectories in particle spectrographs. The method was applied to the correction of several spectrographs, including the S800 under construction at the National Superconducting Cyclotron Laboratory.

ACKNOWLEDGMENTS

For a careful reading of the manuscript and some suggestions, we would like to thank Ralf Degenhardt. This work was supported in part by the U.S. National Science Foundation, Grant No. PHY 89-13815.

[1] J. Nolen, A.F. Zeller, B. Sherrill, J. C. DeKamp, and J. Yurkon, Technical Report No. MSUCL-694, National Superconducting Cyclotron Laboratory, 1989.

[2] A. F. Zeller, J. A. Nolen, L. H. Harwood, and E. Kashy, in *Workshop on High Resolution, Large Acceptance Spectrometers*, Report No. ANL/PHY-81-2, Argonne National Laboratory, 1982.

[3] Conceptual design report, basic experimental equipment, CEBAF Technical report, 1990.

[4] H. A. Thiessen and M. Klein, in Proceedings of the IV International Conference on Magnet Technology, 1972 (unpublished).

[5] Proceedings of the 1991 PILAC Optics Workshop, edited by H. A. Thiessen, Technical Report No. LA-UR-91-3436, Los Alamos National Laboratory, 1991.

[6] Al Zeller, Proceedings of the 1991 PILAC Optics Workshop [5].

[7] M. Berz, COSY INFINITY version 5 reference manual, Technical Report No. MSUCL-811, National Superconducting Cyclotron Laboratory, Michigan State University, East Lansing, MI, 1991.

[8] M. Berz, Nucl. Instrum. Methods, A **298**, 426 (1990).

[9] M. Berz, Part. Accel., **24**, 109 1989.
[10] M. Berz, in *Linear Accelerator and Beam Optics Codes*, Proceedings of a Conference held on Shelter Island, San Diego, CA, 1988, edited by Charles R. Eminhizer, AIP Conf. Proc. No. 177 (AIP, New York, 1989), p. 275.
[11] M. Berz, IEEE Trans. Electron Devices **35**, 2002 (1988).
[12] M. Berz, Nucl. Instrum. Methods A **298**, 473 (1990).
[13] M. Berz, Los Alamos Report No. LA-11857, 1990, p. 137.
[14] M. Berz, Proceedings of the 1991 Particle Accelerator Conference, San Francisco, CA, 1991 (unpublished).
[15] H. Wollnik and M. Berz, Nucl. Instrum. Methods **238**, 127 (1985).
[16] H. G. Blosser, G. M. Crawley, R. DeForest, E. Kashy, and B. H. Wildenthal, Nucl. Instrum. Methods **91**, 197 (1971).
[17] Proceedings of the International Conference on Heavy Ion Research with Magnetic Spectrographs, edited by N. Anantaraman and B. Sherrill, National Superconducting Cyclotron Laboratory, Technical Report No. MSUCL-685, 1989.
[18] H. Enge, in *Focusing of Charged Particles*, edited by A. Septier (Academic, New York, 1967).
[19] H. Wollnik, *Charged Particle Optics* (Academic, Orlando, FL, 1987).
[20] L. C. Teng, Argonne National Laboratory Technical Report No. ANL-LCT-28, 1962.
[21] Ingolf Kübler, Master's thesis, Justus Liebig Universität Giessen, 6300 Giessen, West Germany, 1987.
[22] K. L. Brown and J. E. Spencer, IEEE Trans. Nucl. Sci., **NS-28**, 2568 (1981).
[23] M. Berz, in *Physics of Particle Accelerators*, edited by M. Month (AIP, New York, 1991).
[24] C. Morris, in Proceedings of the International Conference on Heavy Ion Research with Magnetic Spectrographs, National Superconducting Cyclotron Laboratory Technical Report No. MSUCL-685, 1989.